Available online at www.sciencedirect.com
SCIENCE DIRECT®
PERGAMON
International Journal of Heat and Mass Transfer 46 (2003) 2547–2556
International Journal of HEAT and MASS TRANSFER
www.elsevier.com/locate/ijhmt

An experimental study of convective heat transfer in silicon microchannels with different surface conditions

H.Y. Wu, Ping Cheng *

Department of Mechanical Engineering, Hong Kong University of Science and Technology, Clear Water Bay, Kowloon, Hong Kong

Received 31 July 2002; received in revised form 9 January 2003

Abstract

An experimental investigation has been performed on the laminar convective heat transfer and pressure drop of water in 13 different trapezoidal silicon microchannels. It is found that the values of Nusselt number and apparent friction constant depend greatly on different geometric parameters. The laminar Nusselt number and apparent friction constant increase with the increase of surface roughness and surface hydrophilic property. These increases become more obvious at larger Reynolds numbers. The experimental results also show that the Nusselt number increases almost linearly with the Reynolds number at low Reynolds numbers ($Re < 100$), but increases slowly at a Reynolds number greater than 100. Based on 168 experimental data points, dimensionless correlations for the Nusselt number and the apparent friction constant are obtained for the flow of water in trapezoidal microchannels having different geometric parameters, surface roughnesses and surface hydrophilic properties. Finally, an evaluation of heat flux per pumping power and per temperature difference is given for the microchannels used in this experiment.
© 2003 Elsevier Science Ltd. All rights reserved.

Keywords: Convective heat transfer; Microchannels; Roughness; Hydrophilicity

1. Introduction

With the advances of MEMS technology, various silicon-base microsystems such as micro-heat sinks, micro-biochips, micro-reactors, and micro-fuel cells have been developed in recent years. Since microchannels of noncircular cross sections are usually integrated in these silicon-base microsystems, it is important to know the fluid flow and heat transfer characteristics in these microchannels for better design of various microsystems.

Existing experimental results of friction factors and Nusselt numbers in microchannels show that there is a great deal of discrepancies between classical values and the experimental data. Experimental data also appear to be inconsistent with one another. Various reasons have been proposed to account for these differences. One reason may be attributed to various surface conditions, which cannot be neglected in microsystems because of the large surface-to-volume ratio in these systems [1]. For example, the theoretical investigation by Yang et al. [2] and Mala et al. [3] showed that the liquid flow and heat transfer in the rectangular microchannels may be significantly influenced by the presence of the electric double layer near the solid-liquid interfaces.Wu and Little [4] measured the friction factors of gas laminar flow in the trapezoidal silicon/glass microchannels, and found that the surface roughness affected the values of the friction factors even in the laminar flow, which is different from the conventional macrochannel flow. Rahman [5] measured heat transfer in microchannel heat sinks, and obtained larger average Nusselt number than those predicted for larger size channels, which they attributed to the surface roughness associated with the etched channel structure. However, they did not quantify the influence of surface roughness on microchannel heat transfer. Qu et al. [6,7] performed an experimental investigation on pressure drop and heat transfer of water

* Corresponding author. Tel.: +852-2358-7181; fax: +852-2358-1543.
E-mail address: mepcheng@ust.hk (P. Cheng).

0017-9310/03/$ - see front matter © 2003 Elsevier Science Ltd. All rights reserved.
doi:10.1016/S0017-9310(03)00035-8

Nomenclature

A_c	cross-sectional area of the microchannel
A_w	total area of channel bottom wall and side walls
c_p	specific heat of water
$C_{1,2,3}$	correlation factors depending on surface material
D_h	hydraulic diameter of microchannel
f_{app}	apparent friction factor defined in Eq. (1)
$f_{app}Re$	apparent friction constant
f_1, f_2	function
h	average heat transfer coefficient
H	height of microchannel
H/W_t	height-to-top width ratio
k	surface absolute roughness
k/D_h	surface relative roughness
L	length of microchannel
L/D_h	length-to-diameter ratio
M	mass flow rate of water
N	total number of microchannels
Nu	Nusselt number defined in Eq. (8)
Δp	pressure drop across the microchannel
Pr	Prandtl number of water
Q	total heat removed by water
q_p	heat flux per pump power and per temperature difference
Re	Reynolds number of water
$T_1, \ldots, T_5$	longitudinal wall temperature
T_{in}	inlet water temperature
T_{out}	outlet water temperature
ΔT_m	mean temperature difference between water and microchannel wall
$\bar{u}$	mean velocity of water
W_b	bottom width of microchannel
W_t	top width of microchannel
W_b/W_t	bottom-to-top width ratio

Greek symbols

λ	thermal conductivity of water
v	kinetic viscosity of water
θ	channel angle
ρ	density of water

Subscripts

app	apparent
b	bottom
c	cross-section
in	inlet
out	outlet
t	top
w	wall

flow in trapezoidal silicon microchannels. They attributed both the measured higher pressure drops and lower Nusselt numbers to the wall roughness, and proposed a roughness-viscosity model to interpret their experimental data. According to their model, however, the increase in wall roughness caused the decrease in Nusselt number that is contradictory to common sense. The review paper by Meinhart and Wereley [1] pointed out that the fluid transport in nanotubes could be facilitated by decreasing the surface hydrophilic capability, although this novel concept has not been verified experimentally. Ma et al. [8] performed a numerical simulation of microchannel flow over a hydrophilic and hydrophobic surface. They showed that the liquid can remain more easily inside the well of hydrophilic inner surface than that of the hydrophobic inner surface. As far as the authors are aware, however, no published experimental data on the effect of surface hydrophilic property on the convective heat transfer in microchannels has been obtained.

In addition to the various interfacial effects discussed above, the cross-sectional shape of the channel can have great influence on the fluid flow and heat transfer inside the noncircular microchannels as shown by Ma and Peterson's analysis [9], and was confirmed experimentally by Wu and Cheng [10]. Peng and Peterson [11] performed experimental investigations on the pressure drop and convective heat transfer for water flow in rectangular microchannels, and found that the cross-sectional aspect ratio had great influence on the flow friction and convective heat transfer both in laminar and turbulent flows. The effect of cross-sectional aspect ratio on the cooling characteristics of the fluid flow in the rectangular microchannels was also observed by Choi and Cho [12]. Very little experimental data, however, has been published on the effect of the geometric parameters in heat transfer and pressure drop in the trapezoidal microchannels.

For the silicon microchannels used widely in various microsystems, the geometric parameters, the surface roughness, the surface hydrophilic property, and the flow parameters are the important factors affecting the fluid flow and heat transfer characteristics. Depending on the etching method and etching time, two kinds of microchannels (trapezoidal or rectangular microchannels) having different aspect ratios can be fabricated in silicon wafers [13]. Also, various surface roughnesses in the microchannels can be obtained depending on the concentration and temperature of etching solutions [14]. The surface hydrophobic/hydrophilic property can easily be changed by decreasing or increasing the thickness of

oxide layer on a silicon surface [15]. In this paper, the effects of the geometric parameters, the surface roughness, the surface hydrophilic property on pressure drop and heat transfer in microchannels will be clarified. Based on the experimental data, correlations in terms of various affecting factors will be presented for the laminar convective heat transfer and pressure drop in the trapezoidal silicon microchannels. A comparison of heat flux per pumping power and per temperature difference for different microchannels used in this experiment is also obtained.

2. Experimental description

2.1. Experimental setup

Fig. 1 shows the experimental setup used in the present investigation. The deionized water in the high-pressure tank, being pushed by the compressed nitrogen gas, flowed successively through a valve regulator, a filter, a flowmeter, to the test section, and finally was collected by a container. The collecting container was placed on a high precision electronic balance. The mass flow rate of water indicated by the flowmeter was calibrated by the primary measurement of the water mass collected per unit time on the balance. The mass flow rate of water was regulated by the water valve.

The schematic diagram of the test section is also shown in Fig. 1. The silicon chip having parallel microchannels was anodically bonded with a thin pyrex glass plate from the top. The chip was then placed in a teflon base which was attached by a film heater and a thermal-insulating layer at its bottom. The film heater was energized by a DC power supply, which could be regulated in the ranges of 0–220 V and 0–3 A. To measure the wall temperatures, five type-T thermocouples (0.1 mm diameter), being equally spaced from the channel inlet to outlet, were attached at the bottom of the silicon chip. A layer of electric insulation with good heat conduction property was sandwiched between

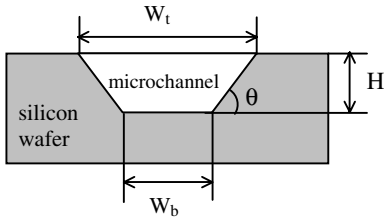

Fig. 2. Cross-section of microchannels.

the wall thermocouples and the film heater. Finally, a polycarbonate plate with liquid inlet and outlet holes was aligned and secured to the teflon base, leaving a leak-proof contact with the pyrex glass through two o-rings. The temperature and pressure of the deionized water at the inlet and outlet of the microchannels were measured by two type-T thermocouples (0.5 mm diameter) and two pressure transducers, respectively. All these measurements along with the measurements of the wall thermocouples were collected and displayed by a PC through a data acquisition system.

The trapezoidal microchannels were formed by wet etching of the $\langle 100 \rangle$ silicon wafers in the solution of KOH. Here, the trapezoidal microchannels were chosen because of its wide application in various microsystems. Moreover, by controlling the concentration, temperature and time of the wet etching, microchannels having different surface roughness and geometric parameters can easily be fabricated, which is essential for the present experimental investigation. Fig. 2 shows the typical cross-sectional shape of the microchannels in the $\langle 100 \rangle$ silicon wafers by wet etching. It can be seen that the triangular channel or rectangular channel is a special trapezoidal channel with $W_b = 0$ or $\theta = 90°$, respectively. Using a surface profiler, the top width W_t, bottom width W_b, and depth H of the trapezoidal microchannels were measured. Also, the surface roughness could be determined using the atomic force microscope (AFM). Table 1 lists the geometric parameters and the surface relative roughness k/D_h of the 13 microchannels used in this

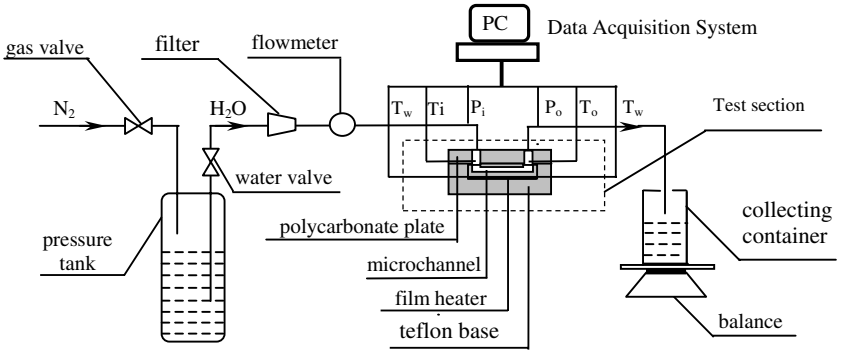

Fig. 1. Experimental setup.

Table 1
Geometric parameters and surface properties of microchannels

Channel no.	W_t (10^{-6} m)	W_b (10^{-6} m)	H (10^{-6} m)	W_b/W_t	H/W_t	k/D_h	L/D_h	Surface material
#1	1473.08	1375.86	56.22	0.934	0.0382	9.85×10^{-5}	285.41	Si
#2	770.48	672.63	56.34	0.873	0.0731	7.59×10^{-5}	298.67	Si
#3	549.83	454.71	56.33	0.827	0.1024	5.69×10^{-5}	310.46	Si
#4	423.2	327.4	56.13	0.774	0.1326	8.63×10^{-5}	325.11	Si
#5	248.83	153.03	56.24	0.615	0.2260	7.64×10^{-5}	370.85	Si
#6	157.99	61.62	56.28	0.390	0.3562	4.30×10^{-5}	453.79	Si
#7	437.21	270.19	110.7	0.618	0.2532	3.26×10^{-5}	191.77	Si
#8	171.7	0	110.8	0	0.6453	3.62×10^{-5}	362.35	Si
#9	429.99	262.30	109.1	0.610	0.2537	5.87×10^{-3}	195.34	Si
#10	168.03	0	108.9	0	0.6481	1.09×10^{-2}	369.29	Si
#11	555.00	459.54	56.77	0.828	0.1023	9.76×10^{-5}	307.90	SiO_2
#12	251.5	155.7	56.50	0.619	0.2247	5.71×10^{-5}	368.11	SiO_2
#13	158.12	62.30	56.49	0.394	0.3573	6.94×10^{-5}	451.40	SiO_2

experiment. To study the effect of surface hydrophilic property on the flow and heat transfer, some silicon microchannels were deposited by a thermal oxide layer of 5000 Å to increase their surface hydrophilic capability. Surface materials for different microchannels are also listed in Table 1.

2.2. Data reduction and error analysis

2.2.1. Flow friction

In this paper, we use the apparent friction factor to evaluate the total pressure drop of the deionized water flowing through the microchannels which is defined as,

$$f_{app} = \Delta p \cdot \frac{D_h}{L} \cdot \frac{1}{2\rho \bar{u}^2} \tag{1}$$

where Δp is the pressure drop measured by the inlet and outlet pressure transducers, ρ is the water density based on the mean value of the inlet and outlet temperatures, D_h and L are the hydraulic diameter and length of the microchannels, and $\bar{u}$ is the average velocity of water obtained from the following equation

$$\bar{u} = \frac{M}{N\rho A_c} \tag{2}$$

where M is the mass flow rate of water, N is the number of microchannels in the chip, and A_c is the cross-sectional area of a microchannel.

The apparent friction constant is defined as the product of the apparent friction factor f_{app} and the Reynolds number Re, i.e.,

$$f_{app}Re = \frac{\Delta p \cdot D_h^2}{2\rho \nu \bar{u} L} \tag{3}$$

where $Re = \bar{u}D_h/\nu$. Substituting Eq. (2) into Eq. (3), we obtain the apparent friction constant in terms of various measurements as

$$f_{app}Re = \frac{\Delta p N A_c D_h^2}{2\nu M L} \tag{4}$$

2.2.2. Heat transfer

In this paper, the heat transfer coefficient for the deionized water flowing through the microchannels is defined by

$$h = \frac{Q}{N A_w \Delta T_m} \tag{5}$$

where A_w is the heat transfer area which is the total area of the side walls and the bottom wall of the microchannel, but it does not include the area of the pyrex glass from the top because it is assumed to be an adiabatic condition. Q is the total heat removed by water which is calculated by

$$Q = Mc_p(T_{out} - T_{in}) \tag{6}$$

The mean temperature difference ΔT_m between the wall and the water is evaluated by

$$\Delta T_m = \frac{1}{5}(T_1 + T_2 + T_3 + T_4 + T_5) - \frac{1}{2}(T_{in} + T_{out}) \tag{7}$$

where, $T_1, T_2, \ldots, T_5$ are the wall temperatures measured by the five wall thermocouples, and T_{in}, T_{out} are the inlet and outlet bulk temperatures of water.

The Nusselt number based on the heat transfer coefficient is given by

$$Nu = \frac{hD_h}{\lambda} \tag{8}$$

where λ is the thermal conductivity of the fluid. Substituting Eqs. (5) and (6) into Eq. (8), we obtain the Nusselt number in terms of various measurements as

$$Nu = \frac{Mc_pD_h(T_{out} - T_{in})}{N\lambda A_w \Delta T_m} \tag{9}$$

Table 2
Measurement errors

Parameters	Maximum errors (%)	Parameters	Maximum errors (%)
D_h	1.88	ρ	0.02
L	0.82	v	2.35
A_c	1.34	c_p	0.02
A_w	1.53	λ	0.31
M	0.98	Re	6.58
Δp	1.11	$f_{app}Re$	10.36
$(T_{out} - T_{in})$	0.73	Nu	7.82
ΔT_m	2.37	–	–

The mean bulk temperature of water $(T_{in} + T_{out})/2$ was used as the characteristic temperature to evaluate the physical properties of the water involved in all above calculations, including the density ρ, kinetic viscosity v, thermal conductivity λ, and specific heat c_p, which are assumed to be independent of pressure.

2.2.3. Error analysis

According to Eq. (4), the error in determining the apparent friction constant $f_{app}Re$ came from the measurement errors of Δp, A_c, D_h, M, L, and v. Also according to Eq. (9), the error in determining the Nusselt number Nu came from the errors of A_w, D_h, M, $(T_{out} - T_{in})$, ΔT_m, c_p and λ. Performing the standard error analysis, the maximum uncertainties in determining Re, $f_{app}Re$ and Nu are presented in Table 2, which also lists the maximum error of various parameters in this study. It can be seen that the errors of $f_{app}Re$ and Nu due to measurement errors in this study were no more than 10.3% and 7.8%, respectively.

3. Experimental results and discussions

From Table 1, it can be conjectured that the Nusselt number and the apparent friction constant are a function of the geometric parameters (W_b/W_t, H/W_t, L/D_h), surface roughness k/D_h, and the surface material. In addition to these factors, the Nusselt number is also a function of the Reynolds number and the Prandtl number of the fluid. Thus,

$$Nu = f_1\left(\frac{W_b}{W_t}, \frac{H}{W_t}, \frac{L}{D_h}, \frac{k}{D_h}, \text{surface material}, Re, Pr\right) \tag{10a}$$

The apparent friction constant is a function of the geometric parameters, surface roughness, surface material, and the Reynolds number, i.e.,

$$f_{app}Re = f_2\left(\frac{W_b}{W_t}, \frac{H}{W_t}, \frac{L}{D_h}, \frac{k}{D_h}, \text{surface material}, Re\right) \tag{10b}$$

The effect of each parameter inside the brackets on the Nusselt number and the apparent friction constant can be shown if other parameters are the same. In the following sections, we will discuss the effects of the surface roughness, surface hydrophilic property, geometric parameters and Reynolds number separately.

3.1. Effect of surface roughness

It is well known that the surface roughness does not affect the laminar flow in macrochannels. However, as the channel size decreases to the order of a few microns, the effect in the surface roughness on the flow and heat transfer of the microchannels becomes important. Figs. 3 and 4 give the experimental results of two pairs of the silicon microchannels with different surface roughness. Microchannels #7 and #9 are two trapezoidal channels having the same geometric parameters ($W_b/W_t = 0.618$–0.610, $H/W_t = 0.2532$–0.2537, $L/D_h = 191.77$–195.34) but different relative surface roughness (3.26×10^{-5}–5.87×10^{-3}), while microchannels #8 and #10 have the triangular cross-section with same geometric parameters but widely different relative surface roughness (3.62×10^{-5}–1.09×10^{-2}). It is shown that at the same Reynolds number, the Nusselt number and apparent friction constant of the trapezoidal microchannel #9 are larger than those of the trapezoidal microchannel #7, which has much lower surface roughness than microchannel 9#. Similar increase in apparent friction constant and Nusselt number is observed for the triangular microchannel #10 ($k/D_h = 1.09 \times 10^{-2}$) which has a higher surface roughness when compared to the triangular microchannel #8 ($k/D_h = 3.62 \times 10^{-5}$). In fact, the surface

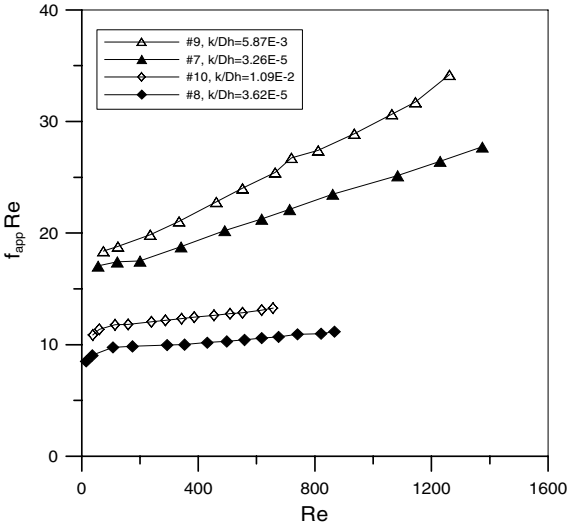

Fig. 3. Effects of surface roughness on apparent friction constant.

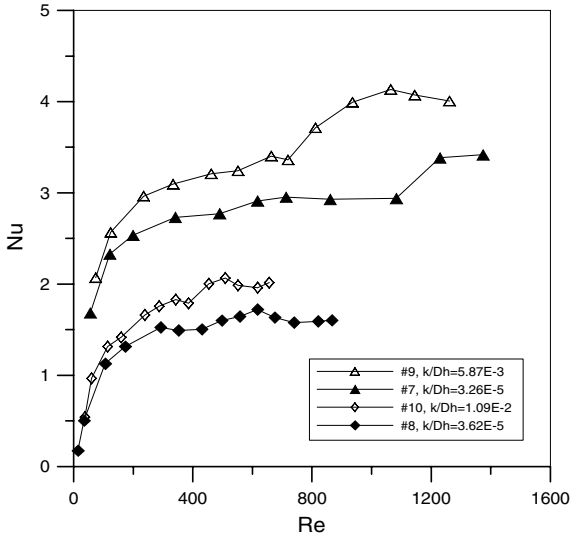

Fig. 4. Effects of surface roughness on Nusselt number.

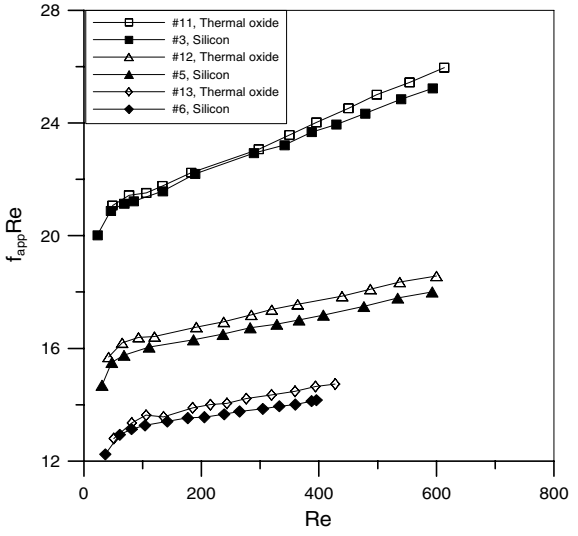

Fig. 5. Effects of surface hydrophilic property on apparent friction constant.

roughness of microchannels #7 and #8 are so small (having order 10^{-5}) that they can be regarded as smooth when compared to the microchannels #9 and #10, whose relative roughness is of the order 10^{-3} or more. It is also found that the Nusselt number and the friction constant of high roughness microchannel increase faster than those of low roughness microchannel with increasing Reynolds number.This is because that the disturbance in the boundary sublayer caused by the roughness is more significant at high Reynolds numbers.

3.2. Effect of surface hydrophilic property

The effects of surface hydrophilic property on the convective heat transfer and flow friction in the microchannels are shown in Figs. 5 and 6, where three sets of data (microchannels #3 and #11, microchannels #5 and #12, microchannels #6 and #13) for the apparent friction constant and the Nussult number are compared. It is pertinent to note that the microchannel pairs of #3 and #11, #5 and #12, #6 and #13 have the same order of roughness respectively. The solid symbols represent the data of the microchannels in the silicon wafer without thermal oxide coatings, while the open symbols represent the data of the microchannels whose silicon surfaces have been coated with a layer of thermal oxide. Note that the thermal oxide surface has a stronger hydrophilic capability than the bared silicon surface [15]. Figs. 5 and 6 show that the Nusselt number and the apparent friction constant of microchannels #11, #12 and #13 (whose surfaces were coated with a thermal oxide layer), are larger than those of the microchannels #3, #5 and #6 (whose surfaces were not coated), respectively. It can be concluded from these experimental results that the increase in the surface hydrophilic capability gives rise to the increase in heat transfer and flow friction inside the microchannels. This is consistent with the analysis by Meinhart and Wereley [1] who showed that the viscous resistance inside nanotubes can be decreased by weakening the surface hydrophilic property.

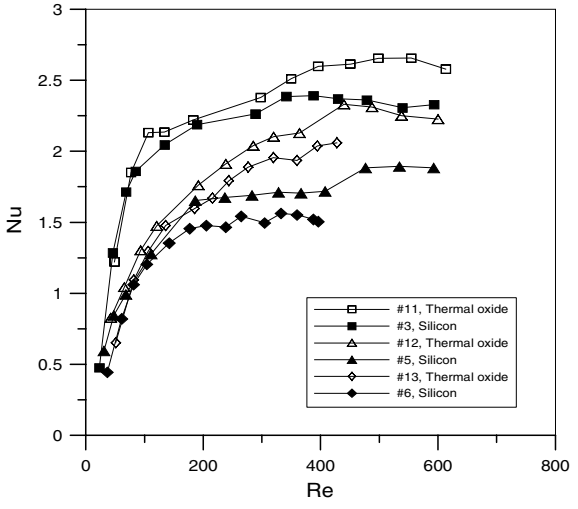

Fig. 6. Effects of surface hydrophilic property on Nusselt number.

3.3. Effect of geometric parameters

It is known that the height-to-width ratio has great effect on the flow friction and heat transfer in the rectangular microchannels [10,11]. For the trapezoidal mi-

crochannel, its cross-sectional shape is determined by two aspect ratios, the height-to-top width ratio H/W_t and the bottom-to-top width ratio W_b/W_t. Therefore, there are three geometric parameters including W_b/W_t, H/W_t and length-to-diameter ratio L/D_h, which affect the friction and heat transfer in the trapezoidal microchannels. Figs. 7 and 8 show the experimental results of microchannels #1 to #6. Since these microchannels were etched under the same conditions in the same silicon wafer, they have approximately the same order of surface roughness (9.85×10^{-5}–4.30×10^{-5}) and same surface hydrophilic property. Thus, the differences in the apparent friction constant and Nusselt number of these microchannels can be attributed to the differences in their geometric parameters W_b/W_t, H/W_t and L/D_h. The results of microchannel #8 were also included in Figs. 7 and 8 to be compared with the data of microchannel #5. It is found that even if the length-to-diameter ratio L/D_h and other conditions are the same, the apparent friction constant and Nusselt number of the microchannels #5 and #8 which have different cross-sectional aspect ratios (W_b/W_t and H/W_t) were much different.

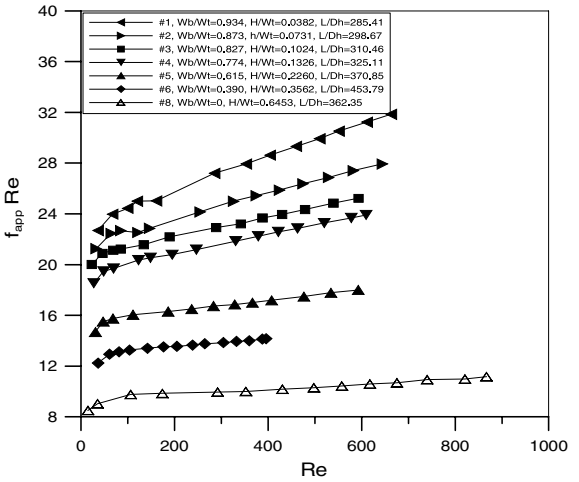

Fig. 7. Effects of geometric parameters on apparent friction constant.

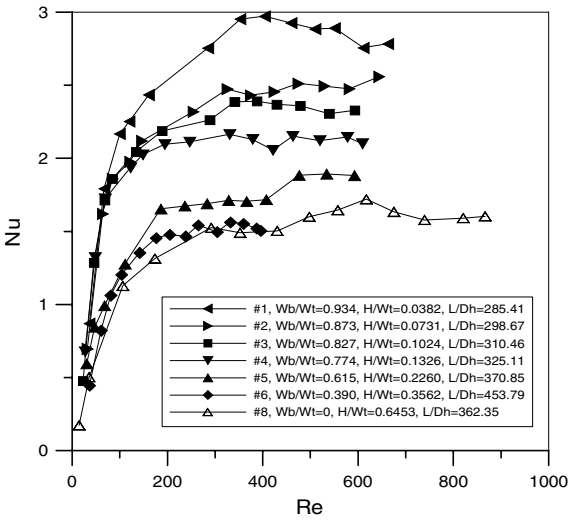

Fig. 8. Effects of geometric parameters on Nusselt number.

3.4. Effect of Reynolds number

From Figs. 3–8, it can be observed that: (1) the Nusselt number and apparent friction constant increased with the increase of Reynolds number; (2) at very low Reynolds numbers ($0 < Re < 100$), the Nusselt number increased drastically with the increase of the Reynolds number; but this increase became much more gently for $Re > 100$; (3) The changes in the Nusselt number and the apparent friction constant due to different geometric parameters, surface roughness and surface hydrophilic property were more obvious at large Reynolds numbers than at low Reynolds numbers. When comparing with the experimental results with those of Peng and Wang [16], it was found that the Nusselt numbers from this experiment have the same order of magnitude as those reported by Wang and Peng [16] although the former are a little higher than the latter. This is probably due to the different definitions of the ΔT_m were used for the definitions of the Nusselt number, and different shape of the microchannels were used.

3.5. Correlations of laminar convective heat transfer

With all factors (H/W_t, W_b/W_t, L/D_h, k/D_h, Re, Pr, and surface material) taken into consideration, the laminar convective heat transfer and friction data for the deionized water flowing through the 13 different trapezoidal microchannels can be correlated in the forms of Eq. (10). The Nusselt numbers are correlated in two separate regimes: $Re < 100$ and $100 < Re < 1500$ as follows:

$10 < Re < 100$

The correlation equation for the Nusselt number in this range of the Reynolds number is

$$Nu = C_1 Re^{0.946} Pr^{0.488} \left(1 - \frac{W_b}{W_t}\right)^{3.547} \left(\frac{W_t}{H}\right)^{3.577} \times \left(\frac{k}{D_h}\right)^{0.041} \left(\frac{D_h}{L}\right)^{1.369} \quad (11a)$$

where C_1 is a factor depending on the surface hydrophilic property: $C_1 = 6.7$ for silicon surfaces and

$C_1 = 6.6$ for thermal oxide surfaces. Thus, the effect of hydrophilic property on Nusselt number is small for $10 < Re < 100$. Eq. (11a) is valid for $4.05 \leqslant Pr \leqslant 5.79$, $0 \leqslant W_b/W_t \leqslant 0.934$, $0.038 \leqslant H/W_t \leqslant 0.648$, $3.26 \times 10^{-4} \leqslant k/D_h \leqslant 1.09 \times 10^{-2}$, and $191.77 \leqslant L/D_h \leqslant 453.79$.

$100 < Re < 1500$

The Nusselt number in this Reynolds number range is correlated as

$$Nu = C_2 Re^{0.148} Pr^{0.163} \left(1 - \frac{W_b}{W_t}\right)^{0.908} \left(\frac{W_t}{H}\right)^{1.001} \times \left(\frac{k}{D_h}\right)^{0.033} \left(\frac{D_h}{L}\right)^{0.798} \tag{11b}$$

where $C_2 = 47.8$ for silicon surfaces and $C_2 = 54.4$ for thermal oxide surfaces. It can be seen that the surface hydrophilic property has significant effects on the Nusselt number for $100 < Re < 1500$. Eq. (11b) is valid for $4.44 \leqslant Pr \leqslant 6.05$, $0 \leqslant W_b/W_t \leqslant 0.934$, $0.038 \leqslant H/W_t \leqslant 0.648$, $3.26 \times 10^{-4} \leqslant k/D_h \leqslant 1.09 \times 10^{-2}$, and $191.77 \leqslant L/D_h \leqslant 453.79$.

Fig. 9 gives the comparison of Eqs. (11a) and (11b) with experimental data. It is shown that the correlations are in reasonable agreement with experimental data. The range of deviations of Eqs. (11a) and (11b) from experimental data are 20.3% and 19.8%, respectively. It is pertinent to note that the vertical coordinates in Fig. 9 are different for the two ranges of the Reynolds number.

3.6. Correlation of the apparent friction constant

The apparent friction factor is correlated by

$$f_{app}Re = C_3 Re^{0.089} \left(1 - \frac{W_b}{W_t}\right)^{4.359} \left(\frac{W_t}{H}\right)^{4.444} \times \left(\frac{k}{D_h}\right)^{0.028} \left(\frac{D_h}{L}\right)^{1.023} \tag{12}$$

where $C_3 = 508.7$ for silicon surfaces and $C_3 = 540.5$ for thermal oxide surfaces. Thus, the thermal oxide surfaces have a higher friction factor than a silicon surface. Eq. (12) is valid when $10 < Re < 1500$, $0 \leqslant W_b/W_t \leqslant 0.934$, $0.038 \leqslant H/W_t \leqslant 0.648$, $3.26 \times 10^{-4} \leqslant k/D_h \leqslant 1.09 \times 10^{-2}$, and $191.77 \leqslant L/D_h \leqslant 453.79$. Fig. 10 is a comparison of the correlation equation given by Eq. (12) with experimental results. It is found that the correlation deviates from experimental data by no more than 19.3%.

3.7. Heat flux per pumping power and per temperature difference

According to the experimental results, the increase of Nusselt number is usually at the expenses of the increase in apparent friction constant. In this paper, we use the heat flux per pumping power and per temperature difference, q_p, to evaluate the performance of different microchannels,

$$q_p = \frac{Q/N}{A_w P \Delta T_m} \tag{13}$$

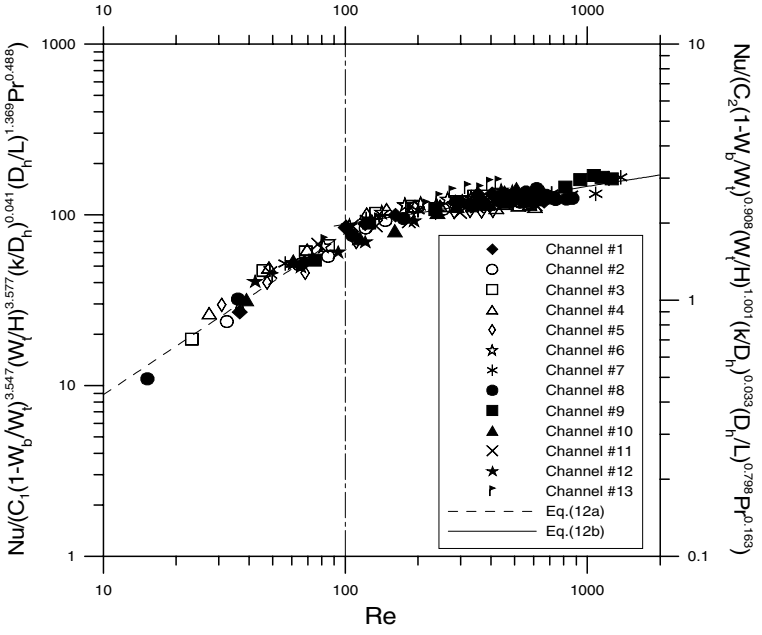

Fig. 9. Comparison of heat transfer correlations with experimental data.

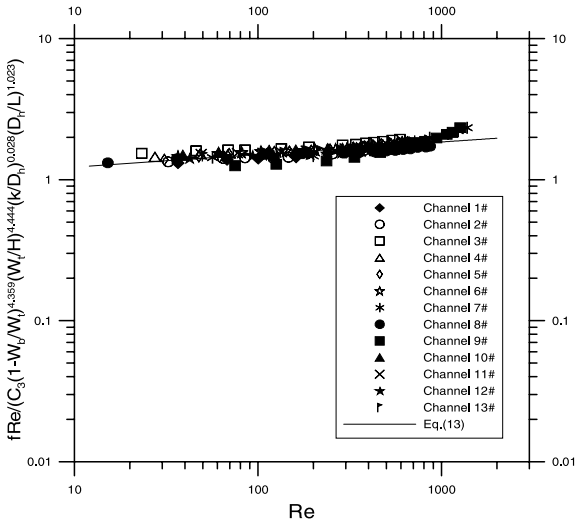

Fig. 10. Comparison of frictin correlation with experimental data.

where P is the pumping power needed to drive the deionized water through the microchannels,

$$P = \Delta P \cdot A_c \cdot \bar{u} \tag{14}$$

Substituting Eqs. (3), (5), (8), and (14) into Eq. (13) and rearranging, we can obtain

$$q_p = \frac{Nu}{f_{app}Re} \cdot \frac{1}{Re^2} \cdot \frac{D_h^3}{LA_c} \cdot \frac{\lambda}{2\rho v^3} \tag{15}$$

Substituting Eqs. (11a), (11b) and (12) into Eq. (13), the values of q_p for different microchannels at various Reynolds numbers can be obtained. Fig. 11 is the comparison of heat flux per pumping power and per temperature difference of the 13 microchannels at the mean water temperature of 30 °C. It can be seen that (1) the performance of microchannels decreased with the rise of Reynolds number in the laminar region; (2) the microchannels #7 and #9 with smaller length-to-diameter ratios had higher values of q_p than other microchannels; (3) by comparing the results of microchannels #7 and #9, as well as microchannels #8 and #10, the surface roughness did not obviously affect the thermodynamic performance; (4) by comparing the results of microchannels #3 and #11, microchannels #5 and #12, and microchannels #6 and #13, the increased in the surface hydrophilic capability caused a small increase in the performance; (5) by comparing the results of all microchannels, it was found that the effect of the geometric parameters (W_b/W_t, H/W_t, L/D_h) on the performance was much more significant than the effects of surface roughness and surface hydrophilic property.

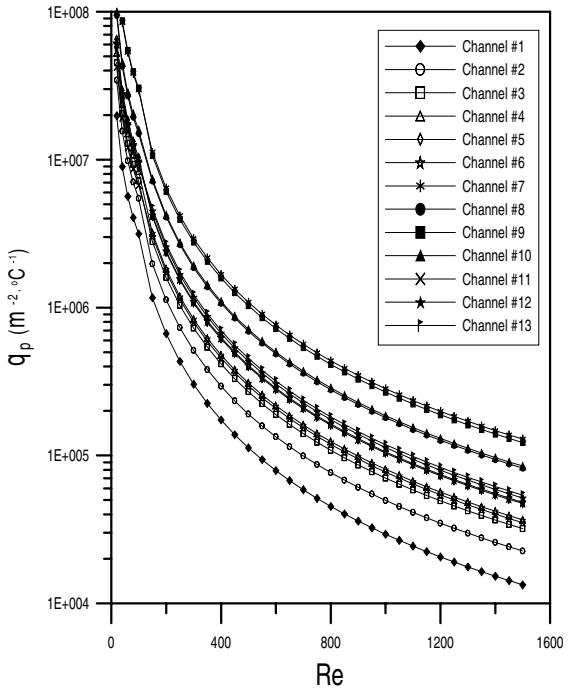

Fig. 11. Heat flux per pumping power and per temperature difference for different silicon microchannels at mean temperature of 30 °C.

4. Concluding remarks

Experimental data of Nusselt number and apparent friction constant for the laminar flow of deionized water through the thirteen trapezoidal microchannels having different geometric paramerters, surface roughness, and surface hydrophilic properties, have been obtained in this paper. The following conclusions are obtained:

1. the bottom-to-top width ratio, the height-to-top width ratio and the length-to-diameter ratio have great effect on the laminar Nusselt number and apparent friction constant of the trapezoidal microchannels;
2. the laminar Nusselt number and apparent friction constant of the trapezoidal microchannels increase with the increase of surface roughness. This increase is more obvious at large Reynolds numbers than that at low Reynolds numbers;
3. the Nusselt number and apparent friction constant of the trapezoidal microchannels having strong hydrophilic surfaces (thermal oxide surfaces) are larger than those having weak hydrophilic surfaces (silicon surfaces). This suggests that convective heat transfer can be enhanced by increasing the surface hydrophilic capability at the expense of increasing pressure drop.

The enhancement in heat transfer is more significant at large Reynolds numbers;

4. the laminar convective heat transfer shows two different characteristics at low and high Reynolds number ranges. For very low Reynolds number flow ($0 < Re < 100$), the Nusselt number increases acutely and almost linearly with the rise of Reynolds number. However, the increase of the Nusselt number after $Re = 100$ is gentle with the rise of the Reynolds number;
5. based on the 168 experimental data points, correlation equations of the Nusselt number and the apparent friction constants in terms of appropriate dimensionless parameters are obtained for the deionized water flowing through the 13 microchannels;
6. heat flux per pumping power and per unit temperature difference is proposed to evaluate the performance of the 13 microchannels used in this experiment. A comparison of results shows that the geometric parameters have more significant effect on the performance than the surface roughness and surface hydrophilic property.

Acknowledgements

The authors gratefully acknowledge the support of this work through grant no. HIA98/99.EG04 and HKUST6014/02.

References

[1] C.D. Meinhart, S.T. Wereley, Fluid mechanics issues at the microscale, in: 39th AIAA Aerospace Sciences Meeting and Exhibition, AIAA 2001-0720, Reno, NV, January 2001.

[2] C. Yang, D.Q. Li, J.H. Masliyah, Modeling forced liquid convection in rectangular microchannels with electrokinetic effects, Int. J. Heat Mass Transfer 41 (24) (1998) 4229–4249.

[3] G.M. Mala, D.Q. Li, C. Werner, Flow characteristics of water through a microchannel between two parallel plates with electrokinetic effects, Int. J. Heat Fluid Flow 18 (5) (1997) 489–496.

[4] P.Y. Wu, W.A. Little, Measurement of friction factors for the flow of gases in very fine channels used for microminiature Joule–Thomson refrigerators, Cryogenics 24 (8) (1983) 273–277.

[5] M.M. Rahman, Measurements of heat transfer in microchannel heat sinks, Int. Commun. Heat Mass Transfer 27 (4) (2000) 495–506.

[6] W.L. Qu, G.M. Mala, D.Q. Li, Pressure-driven water flows in trapezoidal silicon microchannels, Int. J. Heat Mass Transfer 43 (3) (2000) 353–364.

[7] W.L. Qu, G.M. Mala, D.Q. Li, Heat transfer for water flow in trapezoidal silicon microchannels, Int. J. Heat Mass Transfer 43 (21) (2000) 3925–3936.

[8] K.T. Ma, F.G. Tseng, C.C. Chieng, Numerical simulation of micro-channel flow over a well of hydrophilic and hydrophobic surface, in: 39th AIAA Aerospace Sciences Meeting and Exhibition, AIAA 2001-1014, Reno, NV, January 2001.

[9] H.B. Ma, G.P. Peterson, Laminar friction factor in microscale ducts of irregular cross-section, Microscale Thermophys. Eng. 1 (3) (1997) 253–265.

[10] H.Y. Wu, P. Cheng, Friction factors in smooth trapezoidal silicon microchannels with different aspect ratio, Int. J. Heat Mass Transfer, doi:10.1016/S0017-9310(03)00106-6.

[11] X.F. Peng, G.P. Peterson, Convective heat transfer and flow friction for water flow in microchannel structures, Int. J. Heat Mass Transfer 39 (12) (1996) 2599–2608.

[12] M. Choi, K. Cho, Effect of the aspect ratio of rectangular channels on the heat transfer and hydrodynamics of paraffin slurry flow, Int. J. Heat Mass Transfer 44 (1) (2001) 55–61.

[13] M. Madou, Fundamentals of Microfabrication, CRC Press LLC, Boca Raton, FL, 1997, pp. 337–339.

[14] S.W. Kang, J.S. Chen, J.Y. Hung, Surface roughness of $\langle 110 \rangle$ orientation silicon based micro heat exchanger channel, Int. J. Mach. Tools Manufact. 38 (5–6) (1998) 663–668.

[15] S.A.S. Asif, K.J. Wahl, R.J. Colton, The influence of oxide and adsorbates on the nanomechanical response of silicon surfaces, J. Mater. Res. 15 (2) (2002) 546–553.

[16] B.X. Wang, X.F. Peng, Experimental investigation on liquid forced-convection heat transfer through microchannels, Int. J. Heat Mass Transfer 37 (Suppl. 1) (1994) 73–82.